ACS OMEGA

Open Access

http://pubs.acs.org/journal/acsodf

Article

Extraction Process Optimization of Curcumin from *Curcuma xanthorrhiza* Roxb. with Supercritical Carbon Dioxide Using Ethanol as a Cosolvent

Sutarsi, Pundhi T. Jati, Diano Wiradiestia, Ali Altway, Sugeng Winardi, Wahyudiono, and Siti Machmudah*

Cite This: *ACS Omega* 2024, 9, 1251−1264

Read Online

ACCESS | Metrics & More | Article Recommendations

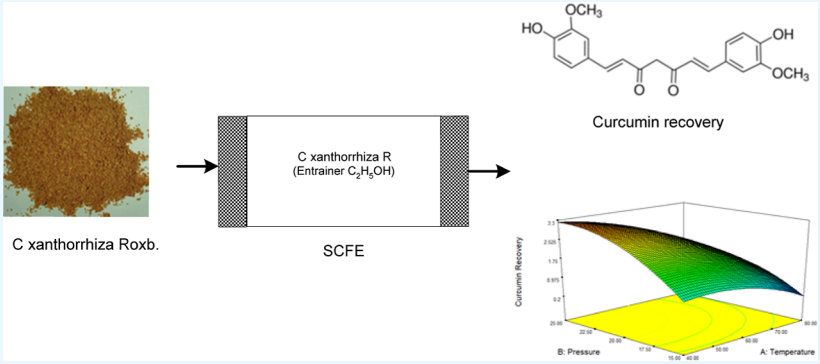

ABSTRACT: *Curcuma xanthorrhiza* Roxb., known as temulawak, Javanese ginger, or Javanese turmeric, is a plant species belonging to the ginger family. This plant originated in Indonesia, more specifically on Java Island, and is usually used as medicine. It contains a high amount of a phenolic compound, namely, curcumin. A supercritical carbon dioxide extraction technique was employed to extract curcumin from *C. xanthorrhiza*. The objective of this work was to investigate the effects of temperature, pressure, and CO_2 flow rate on the extraction yield and curcumin recovery from *C. xanthorrhiza, which* was extracted using supercritical carbon dioxide and ethanol as a cosolvent. The Box−Behnken design (BBD) experimental design and response surface methodology were used to optimize the extraction yield and curcumin recovery. The extraction conditions at a temperature of 40 °C, a pressure of 25 MPa, and a CO_2 flow rate of 5.34 mL/min produced the optimum extraction yield of 10.4% and curcumin recovery of 3.2%. From Fourier transform infrared analysis, although the physical−chemical structure in the residue of the starting material was almost similar, the quantity of all functional groups in the residue decreased from the starting material. From scanning electron microscopy analysis, it was confirmed that the cell was broken due to the high-pressure effect, so that the extraction process runs easily.

INTRODUCTION

Curcuma xanthorrhiza Roxb. is a potential medicinal plant. It belongs to the family Zingiberaceae and the genus Curcuma. It is also called Java turmeric.[1] Although this plant is native to Indonesia,[2] its use has reached many countries in the world and has a long history in traditional care systems.[3] In addition, *C. xanthorrhiza* is used for food coloring, spices, sources of starch, and colorings in cosmetics.[4] The most active and abundant compounds extracted from *C. xanthorrhiza* are essential oil and curcumin.[5] As a natural polyphenol, curcumin is more active as an antioxidant than vitamin E and beta carotene.[6] It is also known for its bioactivities including nitric oxide inhibitory, anti-inflammatory,[7] and anticarcinogenic activities.[8] The need for curcumin is increasing due to the growing awareness of the use of natural products and the rising prices of chemicals. The world demand for curcumin has been filled by *Curcuma longa* (turmeric) extracts from India. India is the world's biggest turmeric producer, with 80% of global production.[9] Indonesia as a tropical country has *C. xanthorrhiza* (temulawak) that can be used as an alternative source of curcumin.

Herbal plants usually have bioactive compounds in low concentrations.[10] There are different methods for the extraction of these compounds from raw materials. Various extraction methods of curcumin have been studied over the last year.[11−15] Organic solvent extraction is the most widely used. The

Received: September 28, 2023
Revised: November 12, 2023
Accepted: December 1, 2023
Published: December 15, 2023

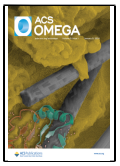

https://doi.org/10.1021/acsomega.3c07497
ACS Omega 2024, 9, 1251−1264

drawback of the organic solvent extraction method is the usage of organic, high-cost solvents, difficult solvent recovery, low selectivity, high impurity, and high environmental impact.[16−19] Therefore, the development of better extraction methods to improve the process, product, and environmental sustainability becomes needed. Environmentally friendly bioactive extraction technology includes extraction with the help of enzymes, microwaves, ultrasound, subcritical water, and supercritical fluids.[20−22]

Supercritical fluid carbon dioxide ($SCCO_2$) extraction has been broadly used for the extraction of bioactive compounds from plant materials. This extraction method uses solvents in supercritical conditions. The unique properties of supercritical liquids make them ideal for use as solvents. Supercritical fluids have high diffusivity, low viscosity, and low surface tension, making them easily penetrable into the material matrix. It has solubility that can be adjusted by changing the operating pressure and temperature. CO_2 is volatile and easily separated to get high-purity products. The solvent can be regenerated easily. Low process temperatures are suitable for thermolabile compounds. It takes a short amount of time with high results and can be joined by other processes. CO_2 is nontoxic, nonflammable, safe for the environment, inexpensive, and available.[23−25] $SCCO_2$ has been used for extractions of phytochemicals from an agro-industrial soybean residue,[26] oats,[27] apple pomace,[28] plants, food byproducts, seaweeds and microalgae,[29] asparagus,[30] and *C. xanthorrhiza*.[31−33]

$SCCO_2$ has shown extraordinary capabilities in the extraction of the essential oils of *Echinophora platyloba*,[34] *Smyrnium cordifolium* Boiss,[35] *Dracocephalum kotschyi*,[36] and *Portulaca oleracea* seed oil.[37] $SCCO_2$ has also shown the capabilities on measuring the solubility of a substance in $SCCO_2$ such as a chemotherapeutic agent (Imatinib mesylate),[38] nilotinib hydrochloride monohydrate (anticancer drug),[39] and buprenorphine hydrochloride.[40] $SCCO_2$ has been employed on the formation of phthalocyanine green nanopigment nanoparticles,[41] Sunitinib malate nanoparticles,[42] sertraline hydrochloride nanoparticles,[43] and amiodarone hydrochloride nanoparticles. $SCCO_2$ has been utilized for the impregnation of lansoprazole loading of polymers,[44] ketoconazole impregnation into polyvinylpyrrolidone and hydroxyl propyl methyl cellulose,[45] optimization and mathematical modeling for the extraction of oil from *D. kotschyi* seeds,[46] extraction of essential oil from *Eryngium billardieri*,[47] and synthesis of cyclic polystyrene.[48]

There are several reports on the application of response surface methodology (RSM) to optimize extraction conditions and thus substantially improve the process efficiency in terms of yield and product composition.[49−54] Salea et al. reported oil and xanthorrhizol extraction from *C. xanthorrhiza* Roxb. rhizome by $SCCO_2$ without cosolvent. The considered factors were temperature, pressure, CO_2 flow rate, and time. Experiments were designed by the Taguchi method. It was optimized using RSM. The result showed that *C. xanthorrhiza* has a high content of ethanol-soluble compounds. As a result, extraction yield from percolation with ethanol as solvent was the highest, and the highest xanthorrhizol content was obtained from $SCCO_2$ at 25 MPa, 50 °C, 15 g/min, and 60 min[33]

The curcumin compound from turmeric has been extracted using modern extraction methods, namely, microwave-assisted, ultrasound-assisted, and enzyme-assisted extraction. The results were compared with those of the traditional extraction method as a standard, namely, Soxhlet extraction. The results showed that the yield of curcumin using Soxhlet was higher than extraction using microwaves (3.72%), ultrasound (3.92%), and enzymes (4.1%).[55] Curcumin and other compounds, namely, demethoxycurcumin and bisdemethoxycurcumin, along with the three main constituents of essential oils, namely, Ar-turmerone, α-turmerone, and β-turmerone, have also been extracted using $SCCO_2$ from *C. longa*.[56,57] There are challenges in this field of pharmacology; apart from being enriched with antioxidants and antimicrobial extracts, more specific research is needed to explore alternative sources of curcumin. Moreover, the optimization of curcumin extraction from *C. xanthorrhiza* using $SCCO_2$, especially to determine the yield and recovery of curcumin, has never been reported in detail.

Furthermore, the purpose of this work was to extract curcumin from *C. xanthorrhiza* using $SCCO_2$ and ethanol as a cosolvent. The efficiency of the process studied was related to the total mass yield (%) and curcumin recovery (%). The experimental design was determined according to Box−Behnken design (BBD). RSM was used to optimize extraction conditions including temperature, pressure, and CO_2 flow rate. The characterization of the product and solid residue was examined.

RESULTS AND DISCUSSION

Curcumin Content in *C. xanthorrhiza*. The curcumin content in the *C. xanthorrhiza* sample was obtained under Soxhlet extraction for 18 h. Even though Soxhlet extraction needs a long period of time and a large amount of organic solvent to extract the target compounds, this method is still the standard extraction method to compare with modern extraction methods such as extraction using $SCCO_2$.[58] 4.8 g of samples was subjected to 250 mL of ethanol. The extract solution was then evaporated using a vacuum rotary evaporator and continued in an oven dryer at a temperature of 40 °C. For curcumin evaluation, the dried extract was redissolved in ethanol. The curcumin content was analyzed by UV−vis spectrophotometry. The result showed that the starting material contained curcumin of 8.08% (g/g sample).

Model Fitting. Dried *C. xanthorrhiza* samples were extracted using $SCCO_2$ to recover curcumin. The observed mass yield and curcumin recovery data are shown in Table 1

Table 1. BBD and Responses for *C. xanthorrhiza* Extraction

run	factors			responses	
	temperature *A*, °C	pressure *B*, MPa	CO_2 flow rate *C*, mL/min	yield, %	curcumin recovery, %
1	60	20	6	7.28	2.59
2	80	20	8	12.60	0.95
3	60	25	8	8.23	0.36
4	80	25	6	8.86	1.39
5	40	20	4	10.08	1.51
6	40	20	8	14.07	1.81
7	60	15	8	10.01	1.63
8	60	20	6	8.73	2.94
9	60	20	6	8.11	2.32
10	80	15	6	14.78	0.16
11	60	15	4	6.86	0.01
12	40	15	6	6.04	1.40
13	80	20	4	6.55	0.21
14	40	25	6	8.39	3.61
15	60	25	4	7.58	1.85

https://doi.org/10.1021/acsomega.3c07497
ACS Omega 2024, 9, 1251−1264

with 15 operating conditions investigated according to the Box−Behnken Design of Experiment (DoE). Including a middle point of the independent variable in every run is a feature in BBD and is beneficial in avoiding operating processes under extreme conditions.[58] Using different starting materials, some studies have applied pressure beyond those used in this study, less than 15 MPa and more than 25 MPa.[59−64]

Curcumin is a natural phenolic compound that features the existence of two hydroxyl functional groups. Curcumin polarity can be explained qualitatively by its chemical structure. The existence of hydroxyl functional groups indicates that curcumin is a polar compound. Therefore, in this study, ethanol was chosen as a cosolvent. In addition, ethanol has low toxicity.

The 15 experiments carried out under the different conditions of independent variables are given in Table 1. There is considerable variation in the extraction yield and curcumin recovery. The extraction yield ranged from 6.04% (run 12) to 14.78% (run 10) and from 0.01% (run 11) to 3.61% (run 14) for curcumin recovery. A regression analysis was employed based on Table 1 using a quadratic model. The model shows the extraction yield and curcumin recovery as a function of temperature, pressure, and flow rate. The estimated extraction yield and curcumin recovery are presented in eqs 1 and 2, respectively.

$$\text{Yield} = -8.44375 - 0{,}257312A + 2.44175B - 0.813750C - 0.020675AB + 0.012875AC - 0.062500BC + 0.005166A^2 - 0.023550B^2 + 0.179688C^2 \quad (1)$$

$$\text{Curcumin recovery} = -31.54292 + 0.120250A + 1.62108B + 4.72437C - 0.002450AB + 0.002750AC - 0.077750BC - 0.001024A^2 - 0.022683B^2 - 0.271771C^2 \quad (2)$$

where A is the temperature, B is the pressure, and C is the CO_2 flow rate.

Analysis of variance (ANOVA) analysis determined the significance of the developed quadratic model. The ANOVA for an estimated quadratic model of the extraction yield is given in Table 2. The quadratic model for the extraction yield is poorly significant with low F-values and high p-values. The model F-value of 1.18 implies that the model is not significant relative to the noise. There is a 45.11% chance that a model F-value this large could occur due to noise.

Values of "Prob > F" less than 0.0500 indicate that model terms are significant. In this case, there are no significant model terms. The lack-of-fit F-value of 19.46 implies that the lack of fit is significant. There is only a 4.93% chance that a lack-of-fit F-value this large could occur due to noise. The significant lack of fit is bad. The correlation coefficient scores, R^2, adjusted R^2, predicted R^2, and adequate precision for eq 1 are 0.6797, 0.1031, −3.9791, and 3.489, respectively. The score of R^2 (0.6797), which is described as the ratio of explained variation to the total variation, ensures a poor fit to the observation data. The difference between adjusted R^2 (0.1031) and predicted R^2 (−3.9791) is 4.0822 (it should be less than 0.20), which indicates a lack of agreement between predicted R^2 and adjusted R^2. The score of adequate precision indicates the adequacy of the signal-to-noise ratio. Furthermore, a poor agreement between the actual and predicted data is given in Figure 1. Hence, the ANOVA of the quadratic model of extraction yield showed that the model was not significant. So, this model cannot be used to navigate the design space.

The ANOVA for a predicted quadratic model of curcumin recovery is given in Table 3. The quadratic model for curcumin recovery has good significance with high F-values and low p-values. The model F-value of 5.20 implies that the model is significant. There is only a 4.21% chance that a model F-value this large could occur due to noise. Values of Prob > F less than 0.0500 indicate that model terms are significant. The lack-of-fit F-value of 4.64 implies that the lack of fit is not significant relative to the pure error. There is an 18.25% chance that a lack-of-fit F-value this large could occur due to noise. A nonsignificant lack of fit is good. The scores of correlation coefficients, R^2, adjusted R^2, predicted R^2, and adequate precision for eq 2 are 0.9034, 0.7296, −0.3783, and 7.843, respectively. The score of R^2 (0.9034), which is defined as a ratio of the described variation to the total variation, ascertains a good fit to the observed data. The difference between adjusted R^2 (0.7296) and predicted R^2 (−0.3783) is 1.1079, which indicates enough agreement between predicted R^2 and adjusted R^2. In addition, a good agreement between the actual and predicted data for curcumin recovery is given in Figure 2. It concludes that the ANOVA for the quadratic model of curcumin recovery showed that the model was significant. So, this model can be used to navigate the design space.

Effect of the Extraction Parameter on the Yield and Curcumin Recovery. The influence of extraction temperature on the extraction yield of *C. xanthorrhiza* at 40, 60, and 80 °C is described in Table 2. Based on ANOVA analysis, extraction temperature has no significant effect on the extraction yield, and it also has no significant effect even with all other parameters (e.g., temperature−pressure, temperature-flow rate).

The effect of extraction pressure on the yield of *C. xanthorrhiza* at 15, 20, and 25 MP is indicated in Table 2. According to ANOVA analysis, extraction pressure has no significant effect on the extraction yield, and it also has no significant effect even with all other parameters (e.g., pressure−temperature, pressure-flow rate).

An extraction flow rate effect on the extraction yield of *C. xanthorrhiza* at 4, 6, and 8 mL/min is demonstrated in Table 2. From ANOVA analysis, it can be determined that the extraction flow rate does not have a significant effect on the extraction yield, and it also has no significant effect even with all other parameters

Table 2. Analysis of Variance of the Estimated Second-Order Polynomial Model for Extraction Yield

source	sum of squares	df	mean square	F value	p-value Prob > F
model	67.80	9	7.53	1.18	0.4511
A—temperature	2.22	1	2.22	0.35	0.5816
B—pressure	2.68	1	2.68	0.42	0.5458
C—flow rate	23.94	1	23.94	3.75	0.1107
AB	17.10	1	17.10	2.68	0.1628
AC	1.06	1	1.06	0.17	0.7005
BC	1.56	1	1.56	0.24	0.6419
$A2$	15.76	1	15.76	2.47	0.1771
$B2$	1.28	1	1.28	0.20	0.6732
$C2$	1.91	1	1.91	0.30	0.6083
residual	31.95	5	6.39		
lack of fit	30.90	3	10.30	19.46	0.0493
pure error	1.06	2	0.53		
cor total	99.76	14			

https://doi.org/10.1021/acsomega.3c07497
ACS Omega 2024, 9, 1251−1264

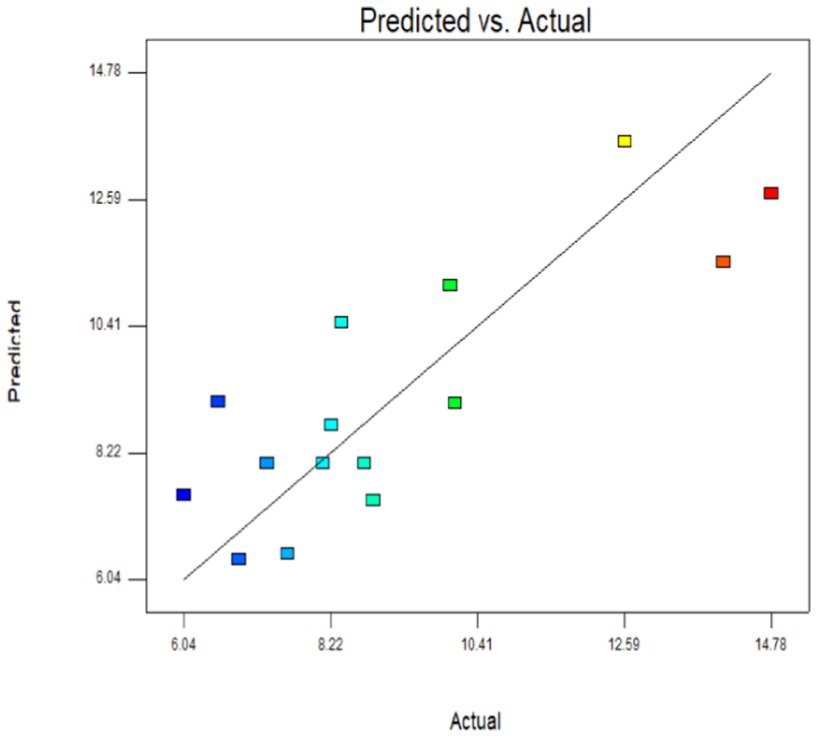

Figure 1. Poor agreement between the actual and predicted data.

Table 3. of the Estimated Quadratic Model for Curcumin Recovery

source	sum of squares	*df*	mean square	*F* value	*p*-value Prob > *F*
model	14.38	9	1.60	5.20	0.0421
A—temperature	3.95	1	3.95	12.84	0.0158
B—pressure	2.01	1	2.01	6.54	0.0509
C—flow rate	0.17	1	0.17	0.56	0.4893
AB	0.24	1	0.24	0.78	0.4174
AC	0.048	1	0.048	0.16	0.7079
BC	2.42	1	2.42	7.86	0.0378
*A*2	0.62	1	0.62	2.01	0.2151
*B*2	1.19	1	1.19	3.86	0.1066
*C*2	4.36	1	4.36	14.19	0.0131
residual	1.54	5	0.31		
lack of fit	1.34	3	0.45	4.64	0.1825
pure error	0.19	2	0.097		
cor total	15.92	14			

(e.g., flow rate-temperature, flow rate-pressure). The results of this study are the same as the results of research conducted by de Andrade Lima et al.;[65] only the linear term of cosolvent concentration significantly affected the extraction. Even though they are not passing the 95%-level threshold set for the experiments, temperature, pressure, and CO_2 flow rate are certainly urgent because they can influence the extraction process to a certain extent.

Based on the results of the ANOVA analysis of the yield prediction model, the *p*-value of the process parameters temperature, pressure, and flow rate is 0.5816, 0.5458, and 0.1107, respectively. A *p*-value greater than 0.05 indicates that temperature, pressure, and flow rate do not have a significant effect on the yield.

Graphically, the effect of individual parameters on the extraction yield can also be known from the perturbation plot in Figure 3. A perturbation plot can only describe an individual effect; it cannot show a parameter interaction effect. The pattern trace followed by a certain parameter describes its sensitivity. A steep slope or curve indicates that the response is sensitive and a flat path indicates that the response is insensitive to that parameter.[66]

Concerning curcumin recovery, the influence of extraction temperature, pressure, and CO_2 flow rate is described in Table 3 (ANOVA). The extraction temperature has a significant effect on the curcumin recovery, and it has no significant interaction effect with all other parameters (e.g., temperature−pressure, temperature-flow rate). Curcumin recovery increases with a decrease in extraction temperature. The decrease in temperature causes an increase in curcumin solubility because of the increasing solvent density.

The *p*-value of the extraction pressure on the curcumin recovery is 0.05. Although it has no significant effect as an individual parameter, it has a significant effect together with other parameters (e.g., pressure-flow rate). Curcumin recovery increases with decreasing pressure. This phenomenon occurs because the decrease in extraction pressure causes a decrease in solvent viscosity, an increase in solvent diffusivity, and an increase in the mass transfer coefficient. Thus, the solvent can penetrate the matrix easily to extract the solute.

According to the ANOVA result, the CO_2 flow rate has no significant effect on the curcumin recovery, but it has a significant effect in conjunction with pressure. Curcumin recovery decreases with an increasing CO_2 flow rate. This phenomenon occurs because an increasing CO_2 flow rate may cause an increasing velocity of fluid to rapidly pass through the extraction bed and exit the extractor under the unsaturated condition. Hence, it causes a decrease in curcumin recovery.[66,67] The effect of individual parameters on curcumin recovery can be confirmed graphically on the perturbation plot in Figure 4.

https://doi.org/10.1021/acsomega.3c07497
ACS Omega 2024, 9, 1251−1264

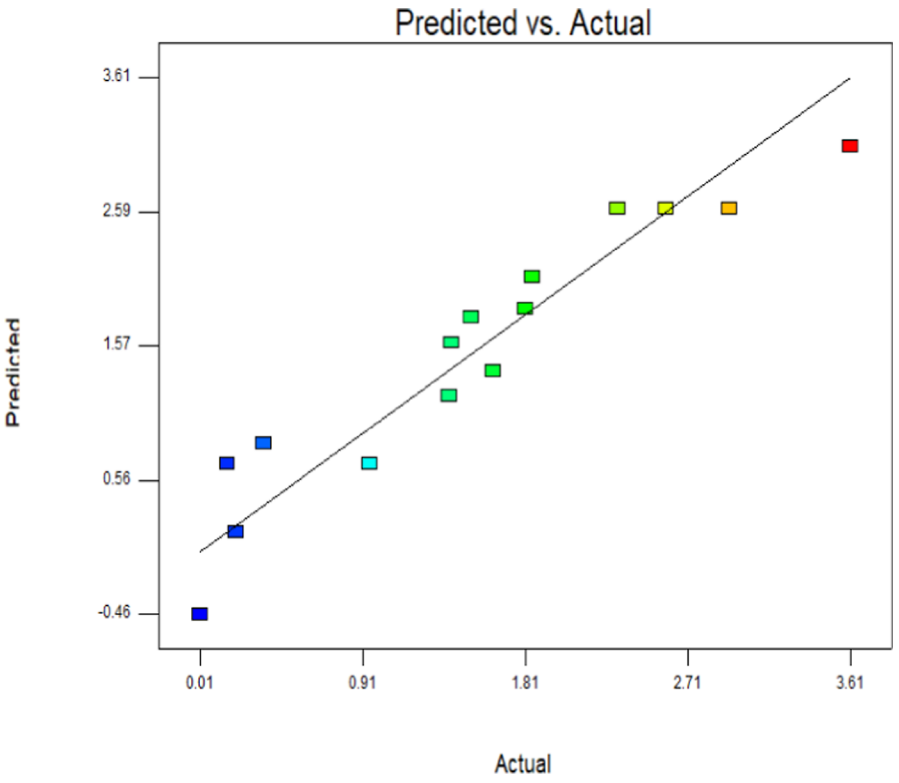

Figure 2. Good agreement between the actual and predicted quadratic models for curcumin recovery.

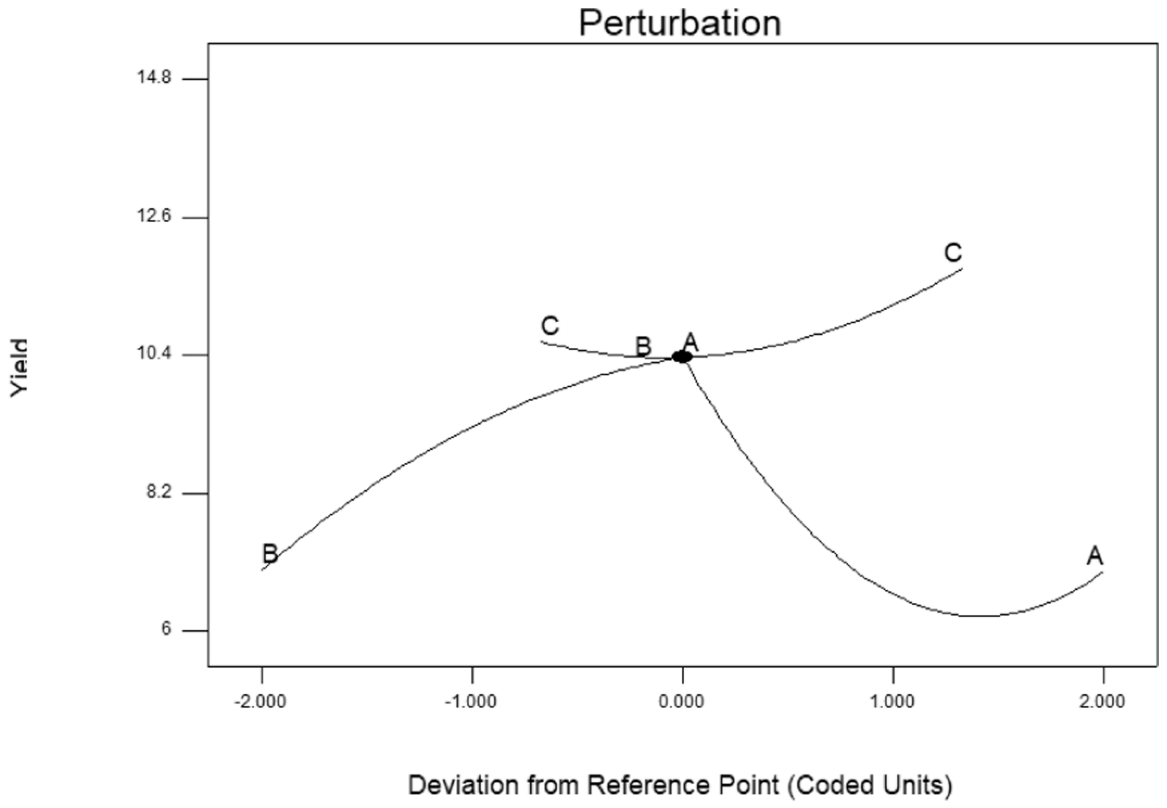

Figure 3. Yield perturbation plot.

Optimal Condition of the Extraction Process. Besides predicting the response variables (extraction yield and curcumin recovery), another purpose of the models is the optimization of operating conditions. The function of extraction optimization is not only to highly increase the extraction yield and curcumin recovery but also to decrease the operational conditions. A three-dimensional (3D) response surface demonstrates the two-extraction parameter interaction on the extraction yield and

https://doi.org/10.1021/acsomega.3c07497
ACS Omega 2024, 9, 1251−1264

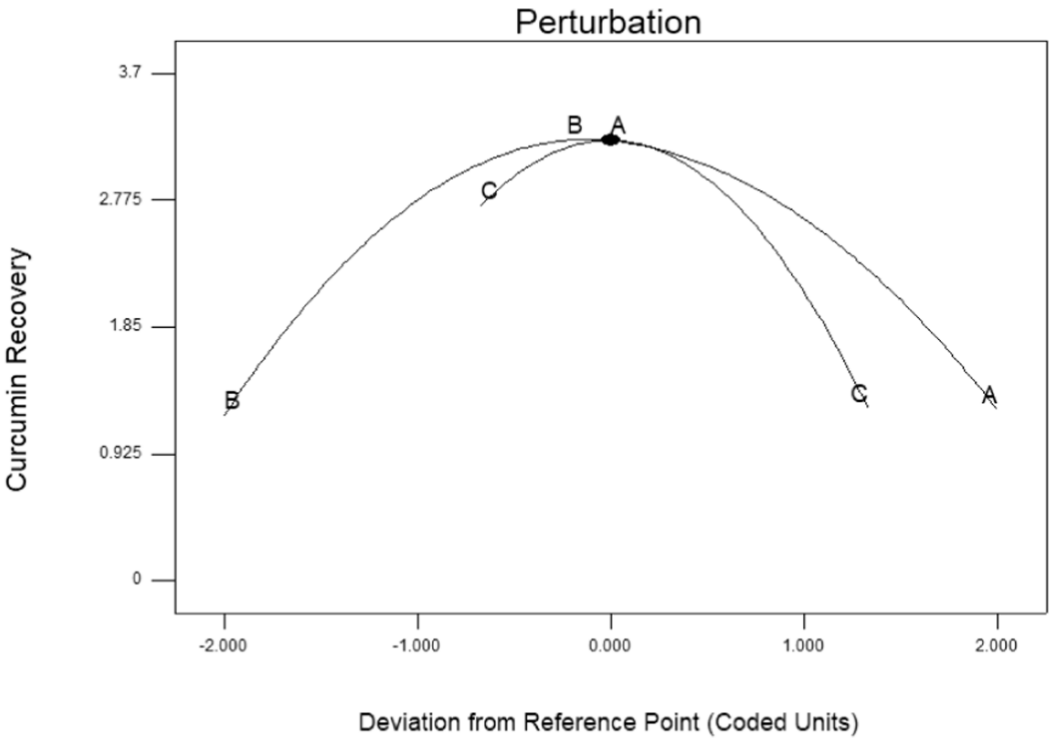

Figure 4. Curcumin recovery perturbation plot.

curcumin recovery. Based on the model indicated in eq 1, the effects of the interaction-independent parameter between temperature, pressure, and flow rate on the extraction yield are shown in Figure 5. According to the result, the optimum extraction yield predicted of 10.4% was obtained at the optimal condition: a temperature of 40 °C, a pressure of 25 MPa, and a CO_2 flow rate of 5.34 mL/min. To validate the predicted optimal conditions, the experiment was conducted under optimal conditions three times. The observed yields were 12.2, 10.7, and 8.5%. The root mean square error (RMSE) was 1.521%. The RMSE value is near 0, which indicates that the model was accurate. The greater the RMSE value, the more the model's validity decreases.

Based on the model indicated in eq 2, the effect of the parameter interaction between temperature, pressure, and flow rate on curcumin recovery is shown in Figure 6. The optimum curcumin recovery of 3.2% was obtained at a temperature of 40 °C, a pressure of 25 MPa, and a CO_2 flow rate of 5.34 mL/min.

A list of studies that work on the optimization of extraction yield and phenolic compound recovery using $SCCO_2$ of various materials with the variable-affecting process is given in Table 4. According to the literature, temperature is the dominant parameter that affects the mass yield and phenolic recovery of biomass extracted using SCFE. The range evaluated in these experiments is generally between 40 and 80 °C.

Pressure has also been shown to affect the extraction in most of the processes, particularly in the range of 10 and 50 MPa. Some exceptions to this are spruce bark waste, citronella grass, carrot peel, and green tea, where pressure does not have a statistically significant effect on the process. Both temperature and pressure have a significant effect on the extraction of radish leaves, *Zea mays* L., green tea scraps, sunflower seed, saffron petal, pinus nigra bark, and *Rosa damascena* Mill.

The cosolvent flow rate has been reported for spruce bark waste, citronella grass, green tea scraps, and carrot peel, and in all cases, there were significant effects on extraction. Other variables that have been investigated and have significant effects are CO_2 flow rate[73,77,78] and extraction time.[73,74,77,78]

Characterization of *C. xanthorrhiza*. Fourier transform infrared spectroscopy (FTIR) is a method used to gain an infrared spectrum of absorption or emission of a solid to study the physicochemical properties of the lignocellulose material. In this section, the FTIR of the starting material and solid residue was compared to determine the effect of $SCCO_2$ extraction. The FTIR spectra of the starting material *C. xanthorrhiza* and $SCCO_2$ extraction residue are depicted in Figure 7. It could be explained clearly that the physicochemical structure of the starting material and residue is almost similar. However, the quantity of all functional groups in the residue decreased from the starting material. It indicates that there is an extraction of the compound during the process. The extraction level of unextracted compounds ≤2.5% is located at wavelengths 1757−2563 and 3593−4000 nm.

Based on the result in Figure 7, the peak spectrum in the region 3600−3000 cm^{-1} with O−H stretching was found in each spectrum. The intensity of these peaks decreased in the residue. The peak at region 1625 cm^{-1} reflects C═C. This indicates that the benzene stretching ring is still found in the solid residue. The peaks at 1152 and 1023 cm^{-1} are due to C−O−C stretching vibration and C−O deformation, respectively. The same result also occurred in the $SCCO_2$ of turmeric; the intensity of these peaks declined in the solid residue.[79]

Table 5 shows the result of gas chromatography−mass spectrometry (GC−MS) analysis for the *C. xanthorrhiza* extract. The extract was mainly composed of ar-turmerone, followed by curlone, gamma-elemene, 3-buten-2-one, 4-(4-hydroxy-3-methoxyphenyl), and other esters or alcohol compounds. Similar to *C. longa*, *C. xanthorrhiza* belongs to the genus Curcuma that mainly contains ar-turmerone.[56]

https://doi.org/10.1021/acsomega.3c07497
ACS Omega 2024, 9, 1251−1264

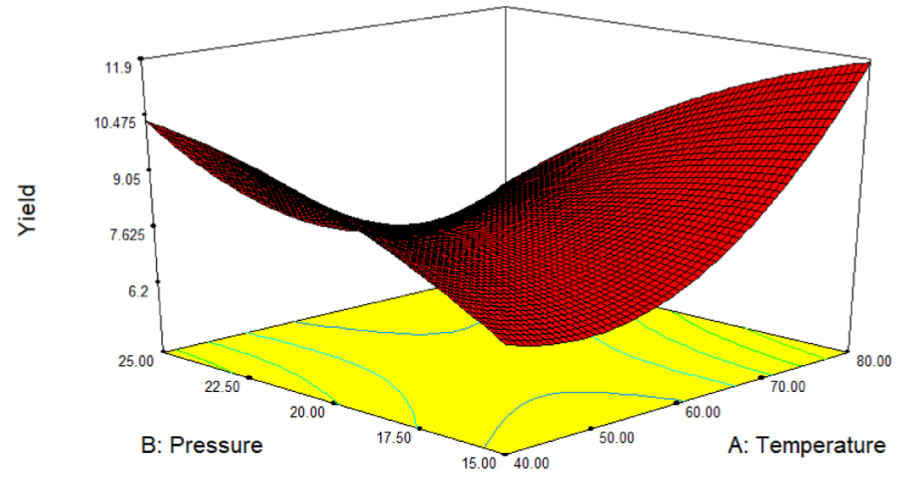

(a)

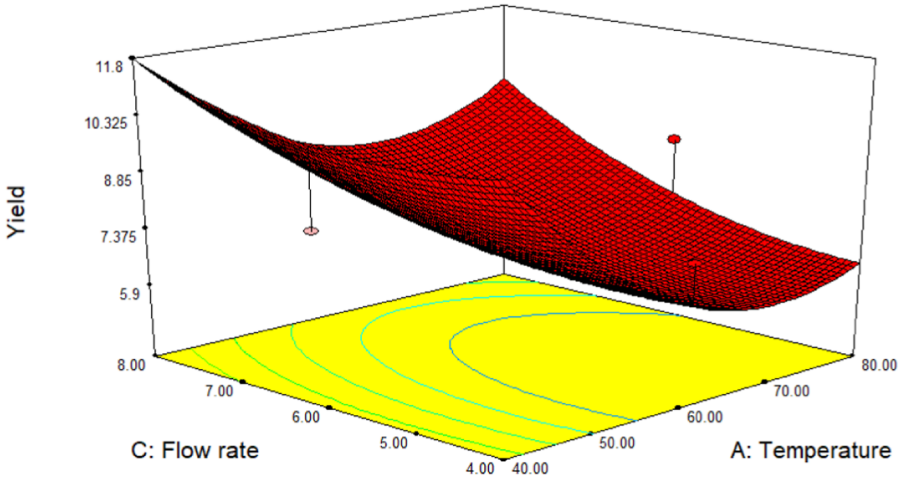

(b)

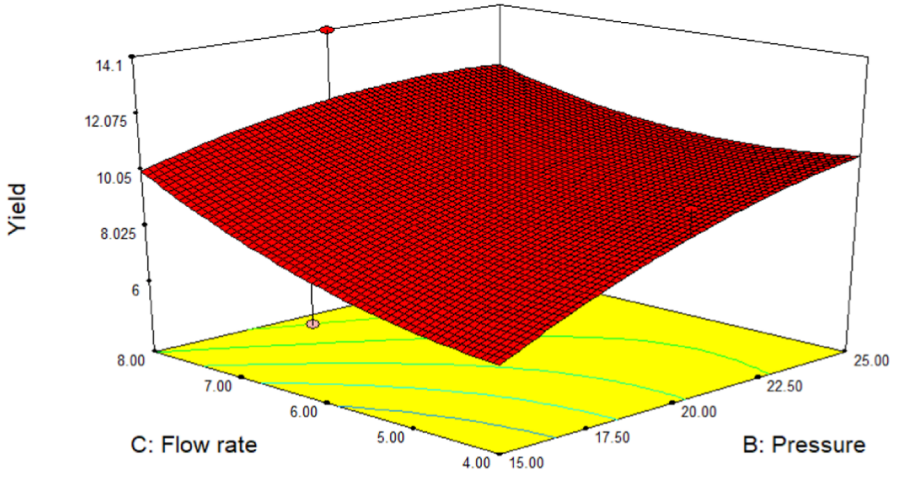

(c)

Figure 5. Interaction-independent parameter between temperature, pressure, and flow rate on the extraction yield.

https://doi.org/10.1021/acsomega.3c07497
ACS Omega 2024, 9, 1251−1264

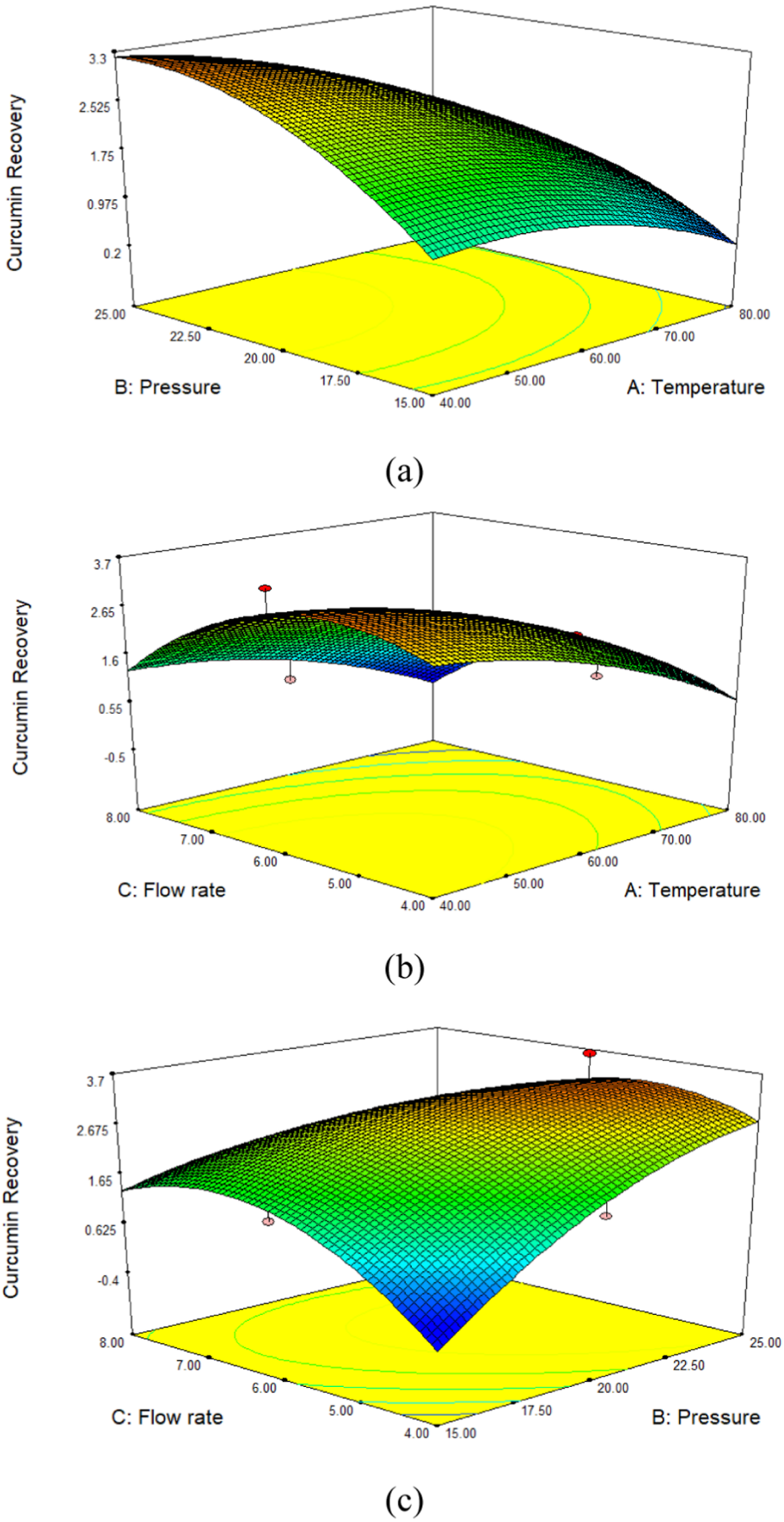

Figure 6. Interaction-independent parameter between temperature, pressure, and flow rate on curcumin recovery.

https://doi.org/10.1021/acsomega.3c07497
ACS Omega 2024, 9, 1251−1264

Table 4. Independent Variable Affecting the Mass Yield and Phenolic Recovery of Various Materials[a]

material	compound of interest	maximum recovery	effect of variable				reference
			T	*P*	*Q*	other	
Mass Yield							
spruce bark waste	mass	30.46 ± 1.20%	x	x		cosolvent flow rate(√)	68
citronella grass	mass	3.76 ± 0.09%	√	x		cosolvent flow rate(√)	69
radish leaves	mass	20%	√	√			70
Zea mays L	mass	10.53%	√	√			71
green tea scraps	mass	23.07 ± 0.82%	√	√		cosolvent flow rate(√)	72
carrot peel	mass	5.4%	x	x		cosolvent flow rate(√)	65
C. xanthorrhiza	mass	10.4%	x	x	x		this work
Phenolic Recovery							
sunflower seed	chlorogenic acid	52.08%	√	√	√	dynamic time (√)	73
O. strictum leaves	TFC	230.48 mg/g	x	√		extraction time (√)	74
green tea	cathecin	2.90%	√	x		cosolvent flow rate (x)	75
saffron petal	TPC	1423 mg/100 g	√	√		extraction time (x)	76
Pinus nigra bark	taxifolin	34 ± 2%	√	√	√	extraction time (√)	77
R. damascena mill	Quercetin	32.0%	√	√	√	extraction time (√)	78
Curcuma longa L.	curcumin	6.9; 3.72; 3.92; 4.1%				Soxhlet, microwave, ultrasonic, enzyme-assisted	55
Curcuma longa L.	curcuminoid, essential oil					LC−MS	56
Curcuma longa L.	turmeric oil			v	v	particle size	57
C. xanthorrhiza Roxb.	curcumin	3.2%	√	√	x		this work

[a]Temperature (*T*), pressure (*P*), CO_2 flow rate (*Q*).

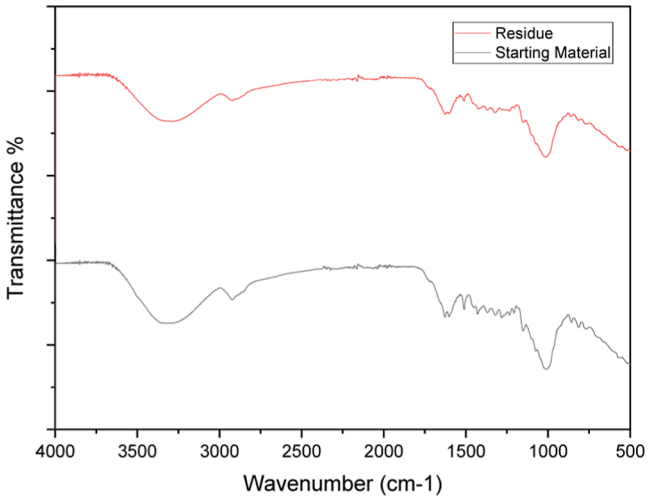

Figure 7. FTIR spectra of the starting material *C. xanthorrhiza* and $SCCO_2$ extraction residue.

Table 5. GS−MS of the *C. xanthorrhiza* Roxb $SCCO_2$ Extract

retention time (min)	component	peak area (%)
36.538	ar-turmerone	19.15
37.515	curlone	7.89
33.46	gamma.-elemene	6.47
40.348	3-buten-2-one, 4-(4-hydroxy-3-methoxyphenyl)	2.74
39.215	3-(2-methyl-[1,3]dithiolan-2-yl)-propionic acid, ethyl ester	1.89
41.059	bicyclo[2.2.1]heptane-7-methanesulfonic acid, 3-bromo-1,7-dimethyl-2-oxo-, [1*R*-(endo,anti)]-	1.85
37.36	1-naphthalenol, decahydro-1,4a-dimethyl-7-(1-methylethylidene)-, [1*R*-(1.alpha.,4a.beta.,8a.alpha.)]-	1.42
39.271	*n*-hexadecanoic acid	1.13
39.404	cyclohexene, 3-(1,5-dimethyl-4-hexenyl)-6-methylene-, [*S*-(*R**,*S**)]-	1.06
44.115	3-methyl-2-butenoic acid, 2-(1-adamantyl)ethyl ester	1.05
37.926	ledene alcohol	1.56

The morphology of the *C. xanthorrhiza* starting material and $SCCO_2$ residue was observed by scanning electron microscopy (SEM) to clearly explain the $SCCO_2$ extraction. The surface morphology of *C. xanthorrhiza* before extraction (Figure 8a) seemed hard and had a little damage on the surface. After $SCCO_2$ extraction (Figure 8b), its cover was damaged and had more pores on the surface. It is shown that the material structure is broken thoroughly because of high-pressure employment. The damage to the cell wall causes the extraction process to be effective. It is confirmed that at high pressure, the cells are broken, and extraction can run easily.[54]

CONCLUSIONS

The BBD experimental design and RSM were used to optimize extraction yield and curcumin recovery. The extraction conditions at a temperature of 40 °C, a pressure of 25 MPa, and a CO_2 flow rate of 5.34 mL/min produced the optimum extraction yield of 10.4% and curcumin recovery of 3.2%. From FTIR analysis, although the physical−chemical structure in the residue of the starting material was almost similar, the quantity of all functional groups in the residue decreased from the starting material. From SEM analysis, it was confirmed that the cell was broken due to the high-pressure effect, so that the extraction process runs easily.

MATERIALS AND METHODS

Chemical Reagents. Liquid analytical carbon dioxide (CO_2, purity of 99.5%) was purchased from Samator, Ltd. (Surabaya, Indonesia). Ethanol (C_2H_5OH, 99.5%), acetonitrile (CH_3CN, 99.8%), orthophosphoric acid (H_3PO_4, 85%), and methanol (CH_3OH, 99.7%) were obtained from Merck (Germany). Curcumin standards were provided by Wako (Osaka, Japan). The mobile phase in high-performance liquid chromatography (HPLC) for curcumin analysis was acetoni-

https://doi.org/10.1021/acsomega.3c07497
ACS Omega 2024, 9, 1251−1264

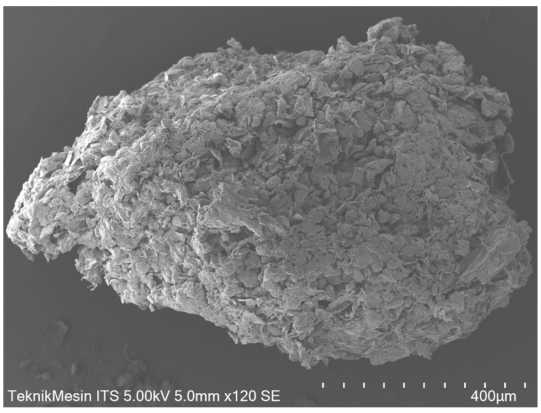

(a)

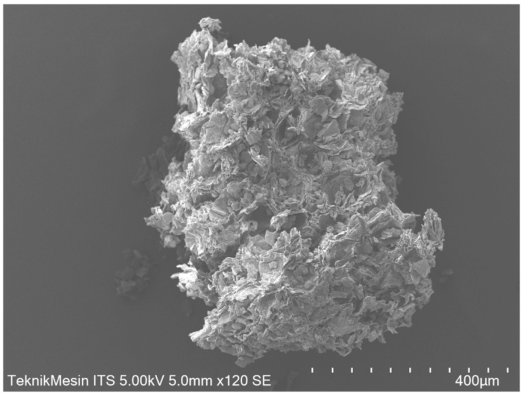

(b)

Figure 8. Structural analysis of *C. xanthorrhiza* Roxb. (a) Before extraction and (b) after $SCCO_2$ extraction.

trile/water/phosphoric acid (50:50:0.5 v/v) with a flow rate of 1 mL/min.[80]

Plant Material. The *C. xanthorrhiza* Roxb. samples were collected from a local market in Jember, East Java, Indonesia. As the starting material, *C. xanthorrhiza* Roxb. was cleaned, sliced, and then oven-dried at 40 °C for 24 h. The moisture content was 12% w/w dry basis, measured by oven drying until a constant weight. The dried rhizome was then ground and sieved to an average diameter particle size of 0.5325 mm.

Extraction Using $SCCO_2$. The supercritical CO_2 extractor unit consisted of a CO_2 line, a recirculating chiller, a HPLC pump (PU-1586, Jasco, Japan), a heating unit (Tokyo Rikakikai, WFO-400, Tokyo, Japan), an extraction vessel (10 mL, Thar Technologies, Inc., PA, USA), a manual back pressure regulator (AKICO, Tokyo, Japan), a collection vial, a pressure gauge, and a flow meter. The schematic diagram of the $SCCO_2$ extractor unit is shown in Figure 9. The extraction process started by turning on the chiller to a temperature of −2 °C to ensure that carbon dioxide became liquid. 2.48 g of the starting material and 2.5 mL of ethanol as a cosolvent were loaded among glass beads into the extractor vessel to prevent channeling. The extractor vessel was then placed on a heating unit in the extractor line. The heating unit was then turned on to the desired temperature of 40, 60, or 80 °C. Carbon dioxide as a solvent was then pumped to a flow rate of 4, 6, or 8 mL/min using a HPLC pump. The extraction system was conditioned above the CO_2 critical pressures of 15, 20, and 25 MPa by adjusting the back pressure regulator (BPR). A heating unit was also installed at the BPR to prevent freezing due to CO_2 expansion when exiting the extraction system. The *C. xanthorrhiza* extract and CO_2 consumption were observed at an extraction time of 240 min. The extract and residue were then analyzed. The yield was calculated by multiplying the ratio of the mass of the extract obtained to the mass of the starting material before extraction by 100%. The curcumin recovery was determined by multiplying the ratio of the curcumin concentration in the extract to the curcumin concentration in the starting material before extraction by 100%.

Experimental Design. To investigate three factors and three levels and optimize the process, the Box−Behnken DoE was used. The three independent factors investigated were pressure (at 15, 20, or 25 MPa), temperature (at 40, 60, or 80 °C), and CO_2 flow rate (Q, at 4, 6, or 8 mL/min). The responses (as dependent variables) investigated were the yield and curcumin recovery. The yield was defined as the % (g/g) of the extracted mass recovered from the starting material mass. Curcumin recovery was defined as the % (g/g) of curcumin mass recovered to the initial curcumin mass in the starting material.

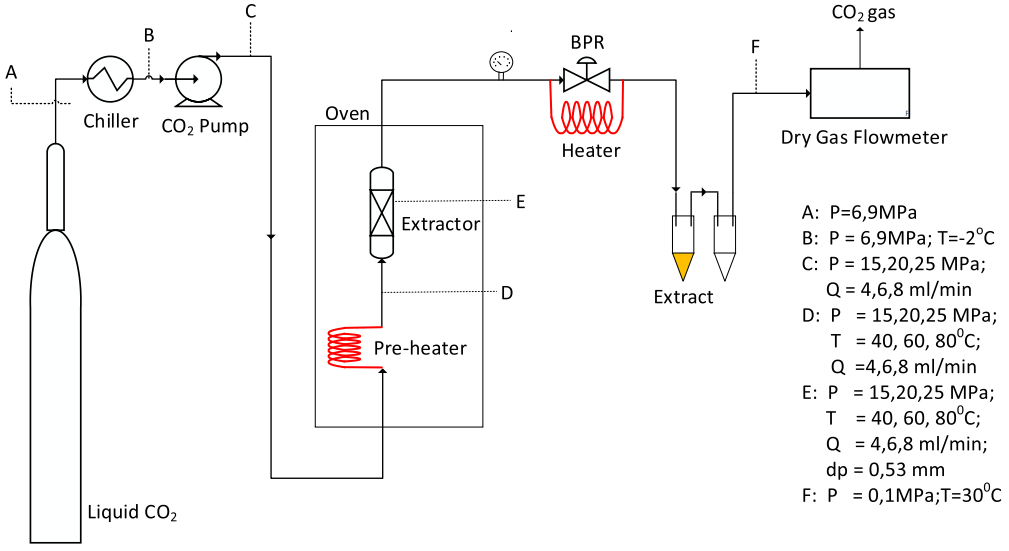

Figure 9. Supercritical CO_2 extractor unit.

https://doi.org/10.1021/acsomega.3c07497
ACS Omega 2024, 9, 1251−1264

Twelve various experiments including low and high parameters were carried out. A central point was replicated three times to determine the experimental errors. The total number of experiments was 15 runs. The extracts obtained were dissolved in ethanol to be taken out from the collection vial for curcumin analysis.

RSM was used for model building and also to determine the optimal extraction conditions. The developed second-order polynomial mathematical model was used to evaluate the relationship between the dependent and the independent variables. Then, the developed mathematical models were used to plot the 3D response surface contour graphs to study the interactive effect of the independent variables on the response, and the validation of the developed models was carried out by plotting an actual versus predicted graph and was examined by ANOVA.[40] Finally, numerical optimization was employed to optimize the $SCCO_2$ extraction process variables for a higher extraction yield and curcumin recovery from *C. xanthorrhiza*.

Statistical Analysis. Regression and response surface evaluation was conducted with Design Expert 7.1.5. Variance analysis (ANOVA was carried out to test the fitness of the model. The generated model was fitted to the observation data by a second-order polynomial model.

$$Y = \beta_0 + \sum_{i=1}^{2} \beta_i X_i + \sum_{i=1}^{2} \beta_{ii} X_i^2 + \sum_{i=1}^{1} \sum_{j=i+1}^{2} \beta_{ij} X_i X_j$$

where Y is the dependent variable, β_0 is the constant, β_i is the linear term coefficient, β_{ii} is the quadratic term coefficient, β_{ij} is the interaction term coefficient, and X_i and X_j are the independent variables.[16]

Curcumin Analysis. The curcumin content in the extract was observed by UV−vis spectrophotometry at a wavelength of 424 nm. A calibration curve was prepared by measuring a standard curcumin solution. The extract solution was diluted with ethanol before analysis. The curcumin concentration in the extract was obtained according to the absorbance of the extract compared to the calibration curve.

The initial curcumin content in *C. xanthorrhiza* was obtained by Soxhlet extraction because this method can extract the curcumin compound from *C. xanthorrhiza* Roxb repeatedly with a pure solvent until all of the target compounds are extracted.

Residue Analysis. The residue was analyzed by Fourier transform infrared resonance and a scanning electron microscope. FTIR was used to determine the presence of molecular functional groups in the residue and starting material. The results were compared to confirm the change in active compounds caused by the extraction process. SEM was done to observe the change of microstructure in the starting material due to the extraction process.[42]

AUTHOR INFORMATION

Corresponding Author

Siti Machmudah − *Department of Chemical Engineering, Institut Teknologi Sepuluh Nopember, Surabaya 60111, Indonesia;* orcid.org/0000-0002-4927-0402; Phone: +62-31-5946240; Email: machmudah@chem-eng.its.ac.id; Fax: +62-31-5999282

Authors

Sutarsi − *Department of Chemical Engineering, Institut Teknologi Sepuluh Nopember, Surabaya 60111, Indonesia;* Present Address: Department of Agricultural Engineering, Fakultas Teknologi Pertanian, Universitas Jember, Jl. Kalimantan 1, Kampus Tegal Boto, Jember 68122, Indonesia

Pundhi T. Jati − *Department of Chemical Engineering, Institut Teknologi Sepuluh Nopember, Surabaya 60111, Indonesia*

Diano Wiradiestia − *Department of Chemical Engineering, Institut Teknologi Sepuluh Nopember, Surabaya 60111, Indonesia*

Ali Altway − *Department of Chemical Engineering, Institut Teknologi Sepuluh Nopember, Surabaya 60111, Indonesia*

Sugeng Winardi − *Department of Chemical Engineering, Institut Teknologi Sepuluh Nopember, Surabaya 60111, Indonesia*

Wahyudiono − *New Industry Creation Hatchery Center, Tohoku University, Aoba-ku, Sendai 980-8579, Japan;* orcid.org/0000-0003-0339-1740

Complete contact information is available at: https://pubs.acs.org/10.1021/acsomega.3c07497

Author Contributions

All authors have given their approval to the final version of the manuscript.

Notes

The authors declare no competing financial interest.

ACKNOWLEDGMENTS

This work was partially supported by Beasiswa Unggulan Dosen Indonesia (BUDI) grant no. PRJ-5468/LPDP.3/2016 and Pascasarjana Research Grant 2019 from Institut Teknologi Sepuluh Nopember (ITS).

ABBREVIATIONS

$SCCO_2$, supercritical carbon dioxide; SEM, scanning electron microscopy; FTIR, Fourier transform infrared spectroscopy

REFERENCES

(1) Nurcholis, W.; Munshif, A. A.; Ambarsari, L. Xanthorrhizol contents, α-glucosidase inhibition, and cytotoxic activities in ethyl acetate fraction of Curcuma zanthorrhiza accessions from Indonesia. *Braz. J. Phcog.* **2018**, *28* (1), 44−49.

(2) Vaiga, R.; Ranggaini, M.; Sandra, F.; Djamil, M. S. Phytochemical and GCMS Profile of Curcuma xanthorrhiza Roxb,. *2017 South East Asian Division Meeting Poster Session 1 Dental Material*; IADR Abstract Archives: Taipei, 2017.

(3) Kholilah, P.; Bayu, R. Aktivitas Farmakologis Zingiber Officinale Rosc., Curcuma Longa L., dan Curcuma Xanthorrhiza Roxb.: Review,. *Farmaka* **2019**, *17* (2), 150−160.

(4) Nadiah Mohammad Rafi, N. S.; Batubara, I.; Steven, A. N. Antibacterial Activity of Leaves and Rhizome of Curcuma xanthorrhiza Essential Oils on Different Distillation Time,. *J. Jamu Indones.* **2018**, *3*, 116−120.

(5) Lukitaningsih, E.; Rohman, A.; Rafi, M.; Af, N.; Windarsih, A. In vivo antioxidant activities of Curcuma longa and Curcuma xanthorrhiza: A review,. *Food Res.* **2019**, *4* (1), 13−19.

(6) Rosidi, A. The difference of Curcumin and Antioxidant activity in Curcuma Xanthorrhiza at different regions,. *J. Adv. Pharm. Educ. Res.* **2020**, *10* (1), 14−18.

(7) Awin, T.; Buzgaia, N.; Abd Ghafar, S. Z.; Mediani, A.; Mohd Faudzi, S. M.; Maulidiani, M.; Shaari, K.; Abas, F. Identification of nitric oxide inhibitory compounds from the rhizome of Curcuma xanthorrhiza. *Food Biosci.* **2019**, *29* (August 2018), 126−134.

(8) Vernieri, C.; Nichetti, F.; Raimondi, A.; Pusceddu, S.; Platania, M.; Berrino, F.; de Braud, F. Diet and supplements in cancer prevention and treatment : Clinical evidences and future perspectives,. *Crit. Rev. Oncol. Hematol.* **2018**, *123* (January), 57−73.

(9) Salma, S.; Aariba, S.; Velvizhi, M.; Yasmin, N.; Sudha, U.; Anitha, M.; Naveena Reddy, S. Qualitative phytochemical analysis of eight turmeric (Curcuma longa L) cultivars grown in various geographical locations of India with six extracts − A comparative study,. *Mater. Today Proc.* **2022**, *66* (May), 909−915.
(10) Soto-Armenta, L. C.; Sacramento-Rivero, J. C.; Ruiz-Mercado, C. A.; Lope-Navarrete, M. C.; Rocha-Uribe, J. A. Extraction yield and kinetic study of Lippia graveolens with supercritical CO2,. *J. Supercrit. Fluids* **2019**, *145*, 205−210.
(11) Sahne, F.; Mohammadi, M.; Najafpour, G. D.; Moghadamnia, A. A. Extraction of bioactive compound curcumin from turmeric (curcuma longa l.) Via different routes: a comparative study,. *Pak. J. Biotechnol.* **2016**, *13* (3), 173−180.
(12) Hadi, B.; Sanagi, M. M.; Wan Ibrahim, W. A.; Jamil, S.; AbdullahiMu'azu, M.; Aboul-Enein, H. Y. Ultrasonic-Assisted Extraction of Curcumin Complexed with Methyl-β-Cyclodextrin,. *Food Anal. Methods* **2015**, *8*, 1373−1381.
(13) Anindya, B.; Anusree, R.; Prosenjit, M.; Tausif, M. A. Curcumin Extraction: Best Solvent On The Basis Of Spectrophotometric Analysis,. *Univers. J. Pharm.* **2015**, *04* (02), 48−52.
(14) Chhouk, K.; Wahyudiono, W.; Kanda, H.; Goto, M. Comparison of Conventional and Ultrasound Assisted Supercritical Carbon Dioxide Extraction of Curcumin from Turmeric (Curcuma longa L.),. *Eng. J.* **2017**, *21* (5), 53−65.
(15) Patil, S.; Shingade, S. M.; Ranveer, R. C.; Sahoo, A. K.; Sahoo, A. K. Optimization of processing conditions for osmotic dehydration of orange segments. *Asian J. Dairy Food Res.* **2018**, *37* (02), 250−252.
(16) Bilgiç-Keleş, S.; Şahin-Yeşilçubuk, N.; Barla-Demirkoz, A.; Karakaş, M. Response surface optimization and modelling for supercritical carbon dioxide extraction of Echium vulgare seed oil,. *J. Supercrit. Fluids* **2019**, *143*, 365−369.
(17) Goyeneche, R.; Di, K.; Ramirez, C. L.; Fanovich, M. A. Recovery of bioactive compounds from beetroot leaves by supercritical CO 2 extraction as a promising bioresource,. *J. Supercrit. Fluids* **2020**, *155*, 104658.
(18) Xie, L.; Cahoon, E.; Zhang, Y.; Ciftci, O. N. Extraction of astaxanthin from engineered Camelina sativa seed using ethanol-modified supercritical carbon dioxide,. *J. Supercrit. Fluids* **2019**, *143* (August 2018), 171−178.
(19) Lima, R. N.; Ribeiro, A. S.; Cardozo-Filho, L.; Vedoy, D.; Alves, P. B. Extraction from Leaves of Piper klotzschianum using Supercritical Carbon Dioxide and Co-Solvents,. *J. Supercrit. Fluids* **2019**, *147*, 205−212.
(20) Cvjetko Bubalo, M.; Vidović, S.; Radojčić Redovniković, I.; Jokić, S. New perspective in extraction of plant biologically active compounds by green solvents,. *Food Bioprod. Process.* **2018**, *109*, 52−73.
(21) Giacometti, J.; Bursać Kovačević, D.; Putnik, P.; Gabrić, D.; Bilušić, T.; Krešić, G.; Stulić, V.; Barba, F. J.; Chemat, F.; Barbosa-Cánovas, G.; et al. Extraction of bioactive compounds and essential oils from mediterranean herbs by conventional and green innovative techniques: A review,. *Food Res. Int.* **2018**, *113* (March), 245−262.
(22) Sagar, N. A.; Pareek, S.; Sharma, S.; Yahia, E. M.; Lobo, M. G. Fruit and Vegetable Waste: Bioactive Compounds, Their Extraction, and Possible Utilization. *Compr Rev Food Sci Food Saf.* **2018**, *17* (3), 512−531.
(23) de O Silva, L.; Ranquine, L. G.; Monteiro, M.; Torres, A. G. Pomegranate (Punica granatum L.) seed oil enriched with conjugated linolenic acid (cLnA), phenolic compounds and tocopherols : Improved extraction of a specialty oil by supercritical CO 2,. *J. Supercrit. Fluids* **2019**, *147* (February), 126−137.
(24) Vatansever, S.; Rao, J.; Hall, C. Effects of ethanol modified supercritical carbon dioxide extraction and particle size on the physical, chemical, and functional properties of yellow pea flour,. *Cereal Chem.* **2020**, *97* (6), 1133−1147.
(25) Santos, K. A.; Klein, E. J.; da Silva, C.; da Silva, E. A.; Cardozo-Filho, L. Extraction of vetiver (Chrysopogon zizanioides) root oil by supercritical CO 2, pressurized-liquid, and ultrasound-assisted methods and modeling of supercritical extraction kinetics,. *J. Supercrit. Fluids* **2019**, *150*, 30−39.
(26) Alvarez, M. V.; Cabred, S.; Ramirez, C. L.; Fanovich, M. A. Valorization of an agroindustrial soybean residue by supercritical fluid extraction of phytochemical compounds,. *J. Supercrit. Fluids* **2019**, *143*, 90−96.
(27) Escobedo-Flores, Y.; Chavez-Flores, D.; Salmeron, I.; Molina-Guerrero, C.; Perez-Vega, S. Optimization of supercritical fluid extraction of polyphenols from oats (Avena sativa L.) and their antioxidant activities,. *J. Cereal Sci.* **2018**, *80*, 198−204.
(28) Ferrentino, G.; Morozova, K.; Mosibo, O. K.; Ramezani, M.; Scampicchio, M. Biorecovery of antioxidants from apple pomace by supercritical fl uid extraction,. *J. Clean. Prod.* **2018**, *186*, 253−261.
(29) Gallego, R.; Bueno, M.; Herrero, M. Sub- and supercritical fl uid extraction of bioactive compounds from plants, food-by-products, seaweeds and microalgae e An update,. *Trends Anal. Chem.* **2019**, *116*, 198−213.
(30) Hasan, M.; Panda, B. P. Chemometric analysis of selective polyphenolic groups in Asparagus racemosus (Shatavar) root extracts by traditional and supercritical fluid (CO 2) based extractions,. *Sep. Sci. Technol.* **2020**, *55* (7), 1339−1355.
(31) Kook, K. E.; Kim, C.; Kang, W.; Hwang, J.-K. Inhibitory Effect of Standardized Curcuma xanthorrhiza Supercritical Extract on LPS-Induced Periodontitis in Rats,. *J. Microbiol. Biotechnol.* **2018**, *28*, 1614−1625.
(32) Kim, S.; Kook, K. E.; Kim, C.; Hwang, J.-K. Inhibitory Effects of Curcuma xanthorrhiza Supercritical Extract and Xanthorrhizol on LPS-Induced Inflammation in HGF-1 Cells and RANKL-Induced Osteoclastogenesis in RAW264.7 Cells,. *J. Microbiol. Biotechnol* **2018**, *28*, 1270−1281.
(33) Salea, R.; Widjojokusumo, E.; Veriansyah, B.; Tjandrawinata, R. R. Optimizing oil and xanthorrhizol extraction from Curcuma xanthorrhiza Roxb. rhizome by supercritical carbon dioxide,. *J. Food Sci. Technol.* **2014**, *51* (9), 2197−2203.
(34) Sodeifian, G.; Sajadian, S. A. Investigation of essential oil extraction and antioxidant activity of Echinophora platyloba DC. using supercritical carbon dioxide,. *J. Supercrit. Fluids* **2017**, *121*, 52−62.
(35) Sodeifian, G.; Azizi, J.; Ghoreishi, S. M. Response surface optimization of Smyrnium cordifolium Boiss (SCB) oil extraction via supercritical carbon dioxide,. *J. Supercrit. Fluids* **2014**, *95*, 1−7.
(36) Sodeifian, G.; Sajadian, S. A.; Saadati Ardestani, N. Supercritical fluid extraction of omega-3 from Dracocephalum kotschyi seed oil: Process optimization and oil properties,. *J. Supercrit. Fluids* **2017**, *119*, 139−149.
(37) Sodeifian, G.; Ardestani, N. S.; Sajadian, S. A.; Moghadamian, K. Properties of Portulaca oleracea seed oil via supercritical fluid extraction: Experimental and optimization,. *J. Supercrit. Fluids* **2018**, *135* (November2017), 34−44.
(38) Sodeifian, G.; Razmimanesh, F.; Sajadian, S. A. Solubility measurement of a chemotherapeutic agent (Imatinib mesylate) in supercritical carbon dioxide: Assessment of new empirical model,. *J. Supercrit. Fluids* **2019**, *146*, 89−99.
(39) Nateghi, H.; Sodeifian, G.; Razmimanesh, F.; Mohebbi Najm Abad, J. A machine learning approach for thermodynamic modeling of the statically measured solubility of nilotinib hydrochloride monohydrate (anti-cancer drug) in supercritical CO2,. *Sci. Rep.* **2023**, *13* (1), 12906−12917.
(40) Sodeifian, G.; Arbab Nooshabadi, M.; Razmimanesh, F.; Tabibzadeh, A. Solubility of buprenorphine hydrochloride in supercritical carbon dioxide: Study on experimental measuring and thermodynamic modeling,. *Arabian J. Chem.* **2023**, *16* (10), 105196.
(41) Saadati Ardestani, N.; Sodeifian, G.; Sajadian, S. A. Preparation of phthalocyanine green nano pigment using supercritical CO2 gas antisolvent (GAS): experimental and modeling,. *Heliyon* **2020**, *6* (9), No. e04947.
(42) Razmimanesh, F.; Sodeifian, G.; Sajadian, S. A. An investigation into Sunitinib malate nanoparticle production by US- RESOLV method: Effect of type of polymer on dissolution rate and particle size distribution,. *J. Supercrit. Fluids* **2021**, *170* (January), 105163.
(43) Sodeifian, G.; Sajadian, S. A.; Derakhsheshpour, R. CO2 utilization as a supercritical solvent and supercritical antisolvent in

https://doi.org/10.1021/acsomega.3c07497
ACS Omega 2024, 9, 1251−1264

production of sertraline hydrochloride nanoparticles,. *J. CO2 Util.* **2022**, *55*, 101799.
(44) Ameri, A.; Sodeifian, G.; Sajadian, S. A. Lansoprazole loading of polymers by supercritical carbon dioxide impregnation: Impacts of process parameters,. *J. Supercrit. Fluids* **2020**, *164*, 104892.
(45) Fathi, M.; Sodeifian, G.; Sajadian, S. A. Experimental study of ketoconazole impregnation into polyvinyl pyrrolidone and hydroxyl propyl methyl cellulose using supercritical carbon dioxide: Process optimization. *J. Supercrit. Fluids* **2022**, *188*, 105674.
(46) Sodeifian, G.; Sajadian, S. A.; Honarvar, B. Mathematical modelling for extraction of oil from Dracocephalum kotschyi seeds in supercritical carbon dioxide,. *Nat. Prod. Res.* **2018**, *32* (7), 795−803.
(47) Sodeifian, G.; Sajadian, S. A.; Saadati Ardestani, N. Experimental optimization and mathematical modeling of the supercritical fluid extraction of essential oil from Eryngium billardieri: Application of simulated annealing (SA) algorithm,. *J. Supercrit. Fluids* **2017**, *127*, 146−157.
(48) Daneshyan, S.; Sodeifian, G. Synthesis of cyclic polystyrene in supercritical carbon dioxide green solvent,. *J. Supercrit. Fluids* **2022**, *188*, 105679.
(49) Sánchez-Camargo, A. d. P.; Gutiérrez, L. F.; Vargas, S. M.; Martinez-correa, H. A.; Parada-alfonso, F.; Narváez-Cuenca, C. E. Valorisation of mango peel: Proximate composition, supercritical fluid extraction of carotenoids, and application as an antioxidant additive for an edible oil,. *J. Supercrit. Fluids* **2019**, *152*, 104574.
(50) Jokić, S.; Molnar, M.; Jakovljević, M.; Aladić, K.; Jerković, I. Optimization of supercritical CO2 extraction of Salvia officinalis L. leaves targeted on Oxygenated monoterpenes, A-humulene, viridiflorol and manool,. *J. Supercrit. Fluids* **2018**, *133*, 253−262.
(51) Rodrigues, V. H.; De Melo, M. M. R.; Silva, C. M. Supercritical fluid extraction of Eucalyptus globulus leaves. Experimental and modelling studies of the influence of operating conditions and biomass pretreatment upon yields and kinetics,. *Sep. Purif. Technol.* **2018**, *191*, 173.
(52) Priyanka; Khanam, S. Influence of operating parameters on supercritical fluid extraction of essential oil from turmeric root,. *J. Clean. Prod.* **2018**, *188*, 816−824.
(53) Derrien, M.; Aghabararnejad, M.; Gosselin, A.; Desjardins, Y.; Angers, P.; Boumghar, Y. Optimization of supercritical carbon dioxide extraction of lutein and chlorophyll from spinach by-products using response surface methodology,. *LWT–Food Sci. Technol.* **2018**, *93*, 79−87.
(54) Campone, L.; Celano, R.; Lisa Piccinelli, A.; Pagano, I.; Carabetta, S.; Sanzo, R. D.; Russo, M.; Ibañez, E.; Cifuentes, A.; Rastrelli, L. Response surface methodology to optimize supercritical carbon dioxide/co-sol- vent extraction of brown onion skin by-product as source of nutraceutical compounds,. *Food Chem.* **2018**, *269*, 495−502.
(55) Widmann, A. K.; Wahl, M. A.; Kammerer, D. R.; Daniels, R. Supercritical Fluid Extraction with CO2 of Curcuma longa L. in Comparison to Conventional Solvent Extraction,. *Pharmaceutics* **2022**, *14* (9), 1943−2017.
(56) Gopalan, B.; Goto, M.; Kodama, A.; Hirose, T. Supercritical carbon dioxide extraction of turmeric (Curcuma longa),. *J. Agric. Food Chem.* **2000**, *48* (6), 2189−2192.
(57) Chang, L. H.; Jong, T. T.; Huang, H. S.; Nien, Y. F.; Chang, C. M. J. Supercritical carbon dioxide extraction of turmeric oil from Curcuma longa Linn and purification of turmerones,. *Sep. Purif. Technol.* **2006**, *47* (3), 119−125.
(58) Ghani, M.; Ghoreishi, S. M.; Masoum, S. Highly porous nanostructured copper oxide foam fiber as a sorbent for head space solid-phase microextraction of BTEX from aqueous solutions,. *Microchem. J.* **2019**, *145*, 210−217.
(59) Shi, J.; Yi, C.; Ye, X.; Xue, S.; Jiang, Y.; Ma, Y.; Liu, D. Effects of supercritical CO 2 fluid parameters on chemical composition and yield of carotenoids extracted from pumpkin,. *LWT–Food Sci. Technol.* **2010**, *43* (1), 39−44.
(60) Mezzomo, N.; Martínez, J.; Maraschin, M.; Ferreira, S. R. S. Pink shrimp (P. brasiliensis and P. paulensis) residue : Supercritical fluid extraction of carotenoid fraction,. *J. Supercrit. Fluids* **2013**, *74*, 22−33.
(61) Vaughn Katherine, L.; Clausen Edgar, C.; King Jerry, W.; Howard Luke, R.; Julie, C. D. Extraction conditions affecting supercritical fluid extraction (SFE) of lycopene from watermelon,. *Bioresour. Technol.* **2008**, *99*, 7835−7841.
(62) Filho, G. L.; De Rosso, V. V.; Meireles, M. A. A.; Rosa, P. T.; Oliveira, A. L.; Mercadante, A. Z.; Cabral, F. A. Supercritical CO 2 extraction of carotenoids from pitanga fruits (Eugenia uniflora L.),. *J. Supercrit. Fluids* **2008**, *46*, 33−39.
(63) Egydio, J. A.; Moraes, Â. M.; Rosa, P. T. V. Supercritical fluid extraction of lycopene from tomato juice and characterization of its antioxidation activity,. *J. Supercrit. Fluids* **2010**, *54*, 159−164.
(64) Döker, O.; Salgın, U.; Şanal, İ.; Mehmetoğlu, Ü.; Çalımlı, A. Modeling of extraction of β-carotene from apricot bagasse using supercritical CO2 in packed bed extractor,. *J. Supercrit. Fluids* **2004**, *28* (1), 11−19.
(65) de Andrade Lima, M.; Charalampopoulos, D.; Chatzifragkou, A. Optimisation and modelling of supercritical CO2 extraction process of carotenoids from carrot peels,. *J. Supercrit. Fluids* **2018**, *133* (September 2017), 94−102.
(66) Suryawanshi, B.; Mohanty, B. Modeling and optimization of process parameters for supercritical CO 2 extraction of Argemone mexicana (L.) seed oil,. *Chem. Eng. Commun.* **2018**, *206* (8), 1087−1106.
(67) Zermane, A.; Larkeche, O.; Meniai, A.; Crampon, C.; Badens, E. Optimization of essential oil supercritical extraction from Algerian Myrtus communis L. leaves using response surface methodology,. *J. Supercrit. Fluids* **2014**, *85*, 89−94.
(68) Talmaciu, A. I.; Ravber, M.; Volf, I.; Knez, Ž.; Popa, V. I. Isolation of bioactive compounds from spruce bark waste using sub- and supercritical fluids. *J. Supercrit. Fluids* **2016**, *117*, 243−251.
(69) Guedes, A. R.; de Souza, A. R. C.; Zanoelo, E. F.; Corazza, M. L.; Corazza, M. L. Extraction of citronella grass solutes with supercritical CO2 compressed propane and ethanol as cosolvent : Kinetics modeling and total phenolic assessment,. *J. Supercrit. Fluids* **2018**, *137* (January), 16−22.
(70) Goyeneche, R.; Fanovich, A.; Rodriguez Rodrigues, C.; Nicolao, M. C.; Di Scala, K. Supercritical CO2 extraction of bioactive compounds from radish leaves: Yield, antioxidant capacity and cytotoxicity,. *J. Supercrit. Fluids* **2018**, *135*, 78−83.
(71) Monroy, Y. M.; Rodrigues, R. A. F.; Sartoratto, A.; Cabral, F. A. Optimization of the extraction of phenolic compounds from purple corn cob (Zea mays L.) by sequential extraction using supercritical carbon dioxide, ethanol and water as solvents,. *J. Supercrit. Fluids* **2016**, *116*, 10−19.
(72) Wang, W.; Han, S.; Zha, X.; Cheng, J.; Song, J.; Jiao, Z. Response Surface Optimization of Supercritical Carbon Dioxide Extraction of Tea Polyphenols from Green Tea Scraps,. *J. AOAC Int.* **2019**, *102* (2), 451−456.
(73) Daraee, A.; Ghoreishi, S. M.; Hedayati, A. Supercritical CO2 extraction of chlorogenic acid from sunflower (Helianthus annuus) seed kernels: modeling and optimization by response surface methodology,. *J. Supercrit. Fluids* **2019**, *144*, 19−27.
(74) Ouédraogo, J. C. W.; Dicko, C.; Kini, F. B.; Bonzi-Coulibaly, Y. L.; Dey, E. S. Enhanced extraction of flavonoids from Odontonema strictum leaves with antioxidant activity using supercritical carbon dioxide fluid combined with ethanol,. *J. Supercrit. Fluids* **2018**, *131*, 66−71.
(75) Sökmen, M.; Demir, E.; Alomar, S. Y. Optimization of sequential supercritical fluid extraction (SFE) of caffeine and catechins from green tea,. *J. Supercrit. Fluids* **2018**, *133*, 171−176.
(76) Ahmadian-Kouchaksaraie, Z.; Niazmand, R. Supercritical carbon dioxide extraction of antioxidants from Crocus sativus petals of saffron industry residues: Optimization using response surface methodology,. *J. Supercrit. Fluids* **2017**, *121*, 19−31.
(77) Ghoreishi, S. M.; Hedayati, A.; Mohammadi, S. Optimization of periodic static-dynamic supercritical CO2 extraction of taxifolin from

https://doi.org/10.1021/acsomega.3c07497
ACS Omega 2024, 9, 1251−1264

pinus nigra bark with ethanol as entrainer,. *J. Supercrit. Fluids* **2016**, *113*, 53−60.
(78) Ghoreishi, S. M.; Hedayati, A.; Mousavi, S. O. Quercetin extraction from Rosa damascena Mill via supercritical CO 2 : Neural network and adaptive neuro fuzzy interface system modeling and response surface optimization,. *J. Supercrit. Fluids* **2016**, *112*, 57−66.
(79) Chhouk, K.; Wahyudiono, W.; Kanda, H.; Goto, M. Comparison of conventional and ultrasound assisted supercritical carbon dioxide extraction of curcumin from turmeric (Curcuma longa L.),. *Eng. J.* **2017**, *21* (5), 53−65.
(80) Pushpakumari, K. N.; Varghese, N.; Kottol, K. Purification and Separation of Individual Curcuminoids from Spent Turmeric Oleoresin, A By-Product fro Curcumin Production Industry,. *Int. J. Pharma Sci. Res.* **2014**, *5* (8), 3246−3254.

https://doi.org/10.1021/acsomega.3c07497
ACS Omega 2024, 9, 1251−1264